Research Article GU J Sci, Part A, 13(2): 849-864 (2026) 10.54287/gujsa.1969621

Gazi University
Journal of Science
PART A: ENGINEERING AND INNOVATION
http://dergipark.org.tr/gujsa

Investigation of Radiation Shielding Parameters of Tantalum Oxide Containing Bismuth Oxide Material

Serra Sude KÖKDUMAN[1] Emre Can HASKİLİT[1*] Sema Bilge OCAK[2,3]

[1] Gazi University, Graduate School of Natural and Applied Sciences, Department of Nuclear Sciences, 06560, Ankara, Türkiye
[2] Gazi University, Graduate School of Natural and Applied Sciences, Department of Advanced Technologies, 06560, Ankara, Türkiye
[3] Gazi University, Basic and Engineering Sciences Central Laboratory Application and Research Center, 06560, Ankara, Türkiye

Keywords

Radiation Shielding
Tantal Oxide
Bismuth Oxide
Lead-free Shielding

Abstract

This study theoretically investigates the radiation shielding performance of epoxy-based composites containing different fractions of bismuth oxide and tantalum oxide as lead-free alternatives. Three composite samples were analyzed using Phy-X/PSD software for photon energies from 1 keV to 105 keV. Results Show that tantalum oxide significantly enhances shielding performance in the medium energy range (70-90 keV) due to tantalum's K-absorption edge at ~67.4 keV, increasing photoelectric interaction probaility. Hybrid composites exhibit broader spectrum shielding compared to single-additive metarials. These epoxy, tantalum oxide and bismuth oxide composite present a promising alternative for portable radiation protection systems and medical imaging devices requiring lead-free shielding materials.

Cite

Kökduman, S. S., Haskilit, E. C., & Ocak, S. B. (2026). Investigation of Radiation Shielding Parameters of Tantalum Oxide Containing Bismuth Oxide Material. *GU J Sci, Part A*, *13*(2), 849-864. doi:10.54287/gujsa.1969621

Author ID (ORCID Number)

0009-0001-9200-1291 Serra Sude KÖKDUMAN
0009-0004-3975-7585 Emre Can HASKİLİT
0000-0002-0590-7555 Sema BILGE OCAK

Article Process

Submission Date 15.06.2026
Revision Date 16.06.2026
Accepted Date 24.06.2026
Published Date 30.06.2026

1. INTRODUCTION

Ionizing radiation is a technology that includes high-energy particles and photons such as gamma rays, X-rays and neutrons, and is now widely used in the fields of medicine, industry, agriculture, and nuclear energy. Especially with the spread of medical imaging systems and the increase in the use of radiation in industrial applications, the issue of radiation safety and armouring has become more critical than ever. The biological effects of ionizing radiation vary depending on parameters such as exposure time, dose level and distance to the source, which requires the development of effective and reliable shielding materials. For this reason, research on understanding the interaction of radiation with matter and designing appropriate shielding solutions is increasing (Şakar et al., 2020).

Gamma rays lose their energy by interacting with matter through different mechanisms such as photoelectric effect, Compton scattering and pair formation (Knoll, 2010) The effectiveness of these interactions is directly related to the atomic number and density of the material (Kaçal et al., 2019). Therefore, materials with a high

*Corresponding Author, e-mail: haskilitemrecan@gmail.com

This work is licensed under Creative Commons Attribution-ShareAlike 4.0 International.

atomic number and density are preferred for radiation shielding. Traditionally, the most widely used material for this purpose is lead. Although lead offers a very effective shielding performance thanks to its high atomic number and density, the need for alternative materials is increasing due to its disadvantages such as toxic structure, damage to the environment, high weight and low melting temperature (Nuñez-Briones et al., 2023). Today, studies for the development of sustainable, environmentally friendly and more human-health safe composite shielding materials come to the forefront (More et al., 2021).

In this context, polymer matrix composites, especially epoxy-based systems, are considered an important alternative in radiation shielding applications. In addition to their advantages such as high mechanical strength, good chemical stability, low density and easy workability, epoxy resins offer a suitable matrix structure that can optimize the armouring performance by allowing homogeneous distribution of additive phases with high atomic numbers. In the literature, there are studies in which the radiation attenuation performance of composites obtained by adding bismuth oxide (Bi_2O_3) in different proportions to the epoxy matrix is examined (Muthamma et al., 2020). Bismuth oxide is one of the prominent materials as an alternative to lead thanks to its high atomic number and relatively low level of toxicity (Khasanov et al., 2026). In addition, bismuth oxide and tantalum oxide composite structures containing PVC are also examined (Nuñez-Briones et al., 2023).

However, radiation attenuation performance is not only closely related to the atomic number and density, but also to the characteristic absorption edges of the elements. At this point, tantalum (Ta) offers a significant advantage. The K-edge of the tantalum at an energy level of about 67.4 keV (Kim et al., 2018) creates a significant jump (absorption edge) around this energy with the possibility of photoelectric absorption. This creates an shielding performance-enhancing effect, especially in low and medium-energy gamma and X-ray applications. On the other hand, the K-edge for bismuth (Bi) occurs at a level of about 90.5 keV (Landsberger et al., 2011) and is active at higher energy ranges. Therefore, the combined use of Bi_2O_3 and Ta_2O_5 allows for an effective radiation absorption performance to be achieved in a wider spectrum by providing a complementary shielding behavior in different energy bands. This synergistic effect offers a significant advantage in terms of optimized composite design, especially in certain energy ranges, such as medical imaging energies.

However, current studies mostly have a single high atomic number additive material and the synergistic effects that can be obtained with the combined use of different additives have not been sufficiently investigated. At this point, tantalum oxide (Ta_2O_5) stands out as another potential additive that attracts attention with its high atomic number, density and chemical stability (Zhang et al., 2021). The use of tantalum oxide with bismuth oxide has the potential to improve not only radiation attenuation performance, but also critical engineering parameters such as mechanical strength, density optimization and cost (Lin et al., 2021).

Currently, many studies focus on discovering lead-free alternative materials and developing lighter and more comprehensive shielding systems. Recent advances in additive manufacturing have further expanded this

scope; Eken et al. (2026) developed bio-based photopolymer–colemanite composites via DLP 3D printing, demonstrating that modern production techniques enable lightweight, sustainable, and effective shielding structures. Similarly, Erdogan et al. (2025) comprehensively investigated Fe-based shape memory alloys and emphasized that radiation shielding evaluation should consider not only photon parameters but also electron and ion interactions. These findings highlight that next-generation shielding materials require a multidimensional approach combining attenuation performance, environmental safety, mechanical properties, and manufacturability (Eken et al,. 2026; Erdogan et al., 2025).

In this study, composite structures containing bismuth oxide (Bi_2O_3) and tantalum oxide (Ta_2O_5) in different fractions in 70% epoxy matrix were theoretically examined in order to develop an alternative armouring material to lead. The goal is to present a composite material design optimized in line with multidimensional criteria such as mechanical strength, density and cost, not only in terms of radiation shielding performance. In this respect, the study offers a more comprehensive approach compared to single-additive epoxy composites in the current literature and aims to develop a new perspective on multi-component composite shield design.

2. THEORY

In this study, photons ranging from 1keV to 105 keV using Phy-X/PSD software Bi_2O_3 for their energies. MAC, LAC, HVL, TVL and Zeff radiation parameters of Ta_2O_5 based alloys were examined.

Mass Attenuation Coefficient (MAC) is the unit area with gamma photons for a specific medium is a quantity that describes the probability of interaction between mass per and can be calculated using Equations (1) and Equation (2) with the well-known Beer-Lambert formula as follows (Şakar et al., 2020);

$$I = I_0 \times e^{-\mu t} \tag{1}$$

$$\mu_m = \left(\frac{\mu}{\rho}\right) = \frac{\ln\left(\frac{I_0}{I}\right)}{\rho t} = \frac{\ln\left(\frac{I_0}{I}\right)}{t_m} \tag{2}$$

I: Attenuated Photon Density, I_0: Unattenuated Photon Density, μ_m: Mass Attenuation Coefficient, t : thickness, t_m: Mass of the sample, ρ: Density are explained by symbols.

Elements with a heavy atomic number show higher values.

The Linear Attenuation Coefficient (LAC) shows how much a material weakens radiation per unit thickness. Its unit is usually cm. The decrease in beam intensity is expressed by the following Equation (1).

Half Value Layer (HVL) and One-Tenth Value Layer (TVL) are the thicknesses required to reduce radiation intensities by half and one-tenth respectively (Şakar et al., 2020). Equation (3) and Equation (4) are calculated using the following;

$$HVL = \frac{\ln(2)}{\mu} = \frac{0.693}{\mu} \quad (3)$$

$$TVL = \frac{\ln(10)}{\mu} = \frac{2.302}{\mu} \quad (4)$$

Mean Free Path (MFP) is the average of a photon before interacting within the material it expresses how far it has come. The following Equation is calculated using (5) (Şakar et al., 2020);

$$MFP = \frac{1}{\mu} \quad (5)$$

The small MFP value means more frequent interaction and better shielding performance.

Effective Atomic Number (Z_{eff}) is the average atomic number in composite materials, which represents the contribution of all components. The high Zeff value provides better shielding, especially in the photoelectric impact zone. Using Equation (6) and Equation (7) can be calculated as follows (Şakar et al., 2020);

$$\sigma_a = \frac{N\mu_m}{N_A} \quad (6)$$

Equation (6) represents the total cross-section area.

where N_A: Avogadro Number, μ_m: Mass Attenuation Coefficient, N: Atomic Mass

$$\sigma_e = \frac{1}{N_A} \quad (7)$$

Equation (7) refers to the total electronic section. The combined use of these expressions can be calculated with the following Equation (8);

$$Z_{eff} = \frac{\sigma_a}{\sigma_e} \quad (8)$$

The densities of the components are a direct effective parameter in radiation shielding. The fraction is calculated by mass for all composites used in this article. This theoretical density using the rule of mixtures can be calculated with the Equation (9);

$$\frac{1}{\rho_{comp}} = \frac{w_1}{\rho_1} + \frac{w_2}{\rho_2} + \frac{w_3}{\rho_3} \quad (9)$$

W_i: percentage by mass of component number i, ρ_i: density of component number i

$$\sum_R = \sum_i \rho_i (\Sigma_R/\rho)_i \quad (10)$$

The fast neutron removal cross-section (Σ_R) is a fundamental shielding parameter that represents the probability per unit path length of a fast neutron being removed from the fast energy group following initial interactions. For composite materials, this value is determined by weighting the mass removal cross-sections $(\Sigma_R/\rho)_i$ of each constituent by their partial densities (ρ_i) in accordance with the additivity rule.

The a, b, c, d and Xk symbols used in the G-P compatibility parameters for EBF are below defined. (Harima, 1983)

$$B(E,x) = 1 + K - 1(b-1)(Kx-1) \quad for\,\mathrm{K} \neq 1 \tag{11}$$

$$B(E,x) = 1 + (b-1)x \quad \text{for K} = 1 \tag{12}$$

Here B accumulation factor, E photon energy, x thickness in MFP, b G-P fitting parametets. K is the coefficient obtained from other parameters.(Singh & Badiger, 2015)

$$K(E,x) = cX^a + d\frac{(\tanh(-2)\tanh(x/Xk-2) - \tanh(-2))}{1-\tanh(-2)} \tag{13}$$

for penetration depth (X) ≤ 40 mfp

B:1 is the accumulation factor value at the average free path (1 mfp) distance. It determines the initial trend. C and a: They are the coefficients that determine the character of the K factor (distance-dependent increase rate) at low depths. Xk: It is the reference depth of the radiation "changes characteristic behavior" in the matter or the tendency of the accumulation factor changes, depending on the atomic structure of the material. d: It is the correction coefficient used to correct saturation or deviations at high depths (often above the Xk value). (Singh & Badiger, 2015) The sample nomenclature and the mass percentages of the components are presented in Table 1.

Table 1. *Naming and contents of samples*

Naming of samples	***$C_{18}H_{19}O_3$* (Mass %)**	***Bi_2O_3* (Mass %)**	***Ta_2O_5* (Mass %)**	***ρ* (g/cm^3)**
S1	70	30	0	1,653
S2	70	15	15	1,654
S3	70	5	25	1,653

The advantage of composites containing tantalum oxide (Ta_2O_5) in terms of material selection is due to the characteristic absorption edge behavior of elements with high atomic numbers. The photoelectric effect is the dominant mechanism in the low energy range, and this interaction strongly depends on the atomic number and photon energy. K-absortion of tantalum at approximately 67.4 keV the edge causes a significant increase in photoelectric absorption at photon energies around 80 keV. On the other hand, this contribution is not yet fully activated due to the higher K-edge of bismuth (~90.5 keV) in the same energy range. This allows hybrid composites containing Ta_2O_5 to exhibit a higher mass absorption coefficient in the energy region in question

and their attenuation behavior to be more controlled (softer inclined). At higher energies, with the dominance of the Compton scattering mechanism, the effect of the material composition decreases and similar attenuation trends are observed. In this context, the Ta_2O_5 contribution offers the advantage of a significant material selection that improves shielding performance, especially in the medium energy range (=70-90 keV). The variation of radiation shielding parameters with incident photon energy is presented in Figure 1 through 6. Specifically, the MAC and LAC are shown in Figure 1 and 2, while the HVL, TVL, Z_{eff}, and FNRCS are depicted in Figure 3, 4, 5, and 6, respectively. Furthermore, the G-P fitting parameters for samples S1, S2, and S3 at various energy levels are presented in Table 2, 3, and 4, respectively.

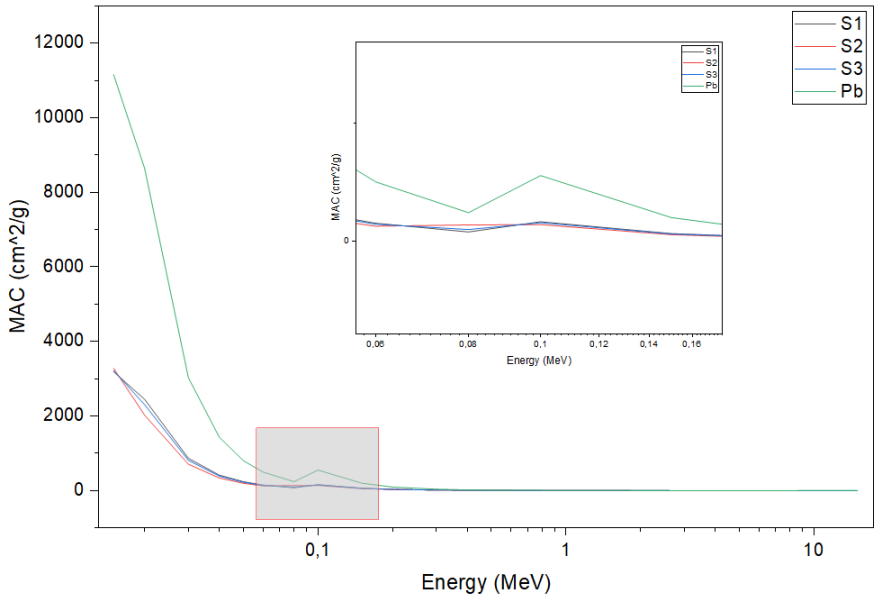


Figure 1. *MAC-Energy graph of S1, S2 and S3 samples*

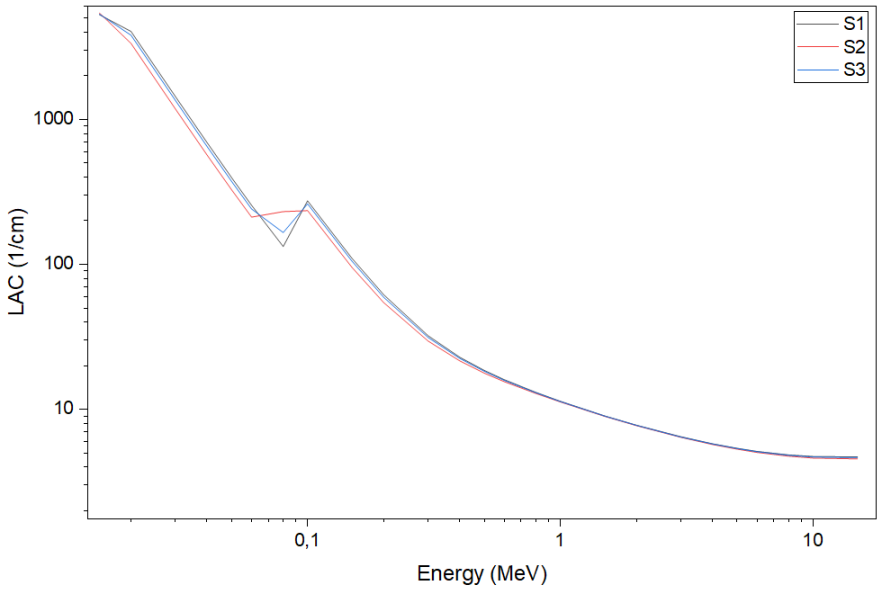


Figure 2. *LAC-Energy graph of S1, S2 and S3 samples*

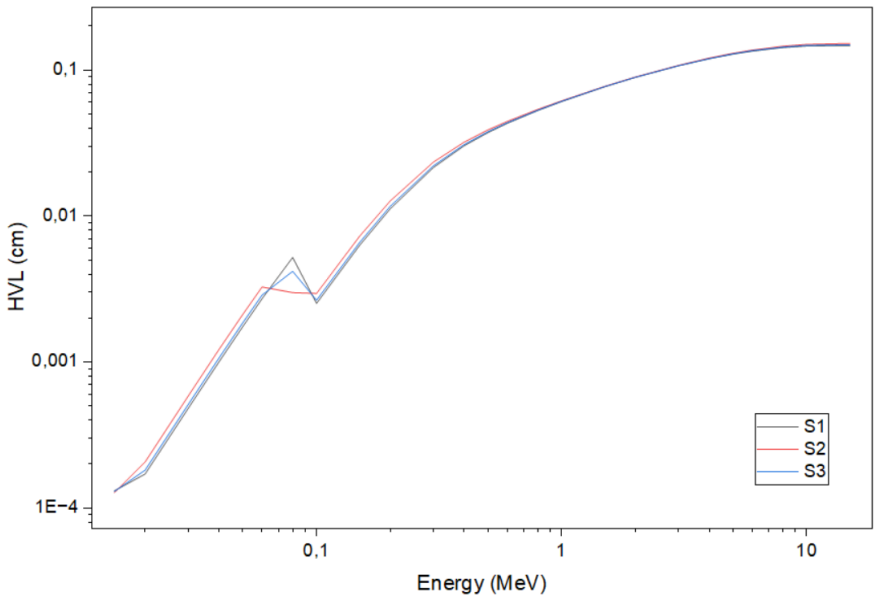


Figure 3. *HVL-Energy graph of S1, S2 and S3 samples*

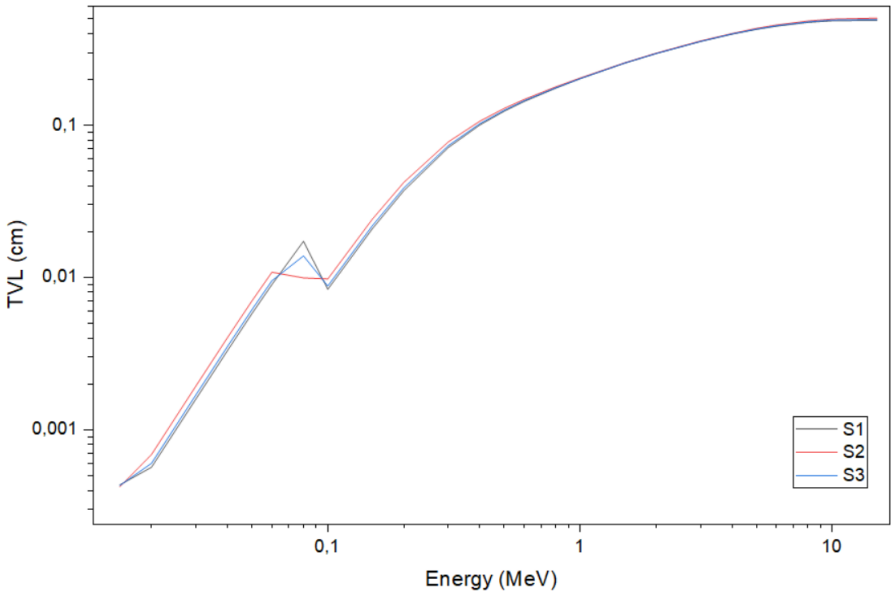


Figure 4. *TVL-Energy graph of S1, S2 and S3 samples*

The analysis results show that the fast neutron armouring ability systematically improves as the tantalum ratio in the mixture increases. This linear correlation confirms that the probability of tantalum interacting with rapid neutrons is higher than bismuth substitutes and positively affects the macroscopic effect cross-section. This performance advantage of tantalum reinforced epoxy systems over conventional lead-based shield paves the way for highly efficient and lead-free new generation shield designs in radiation safety applications.

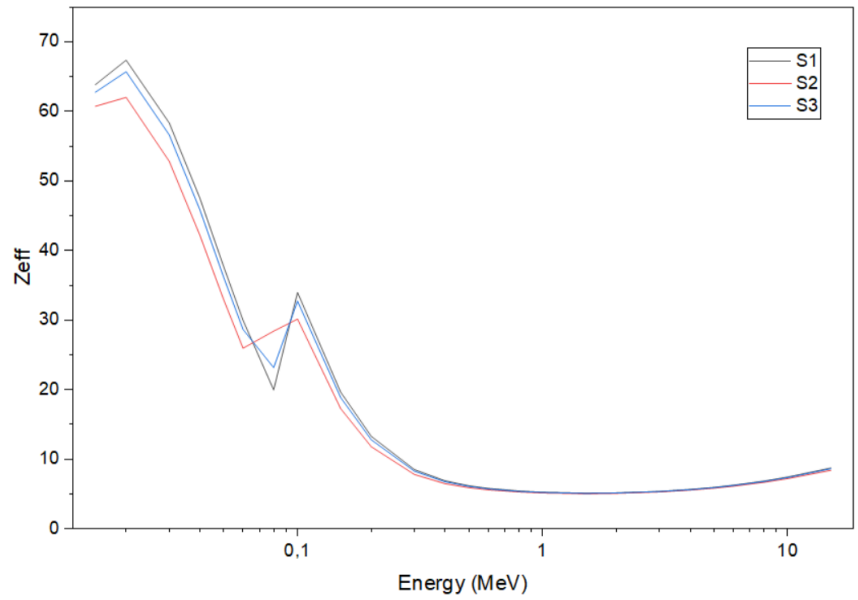


Figure 5. *Zeff-Energy graph of S1, S2 and S3 samples*

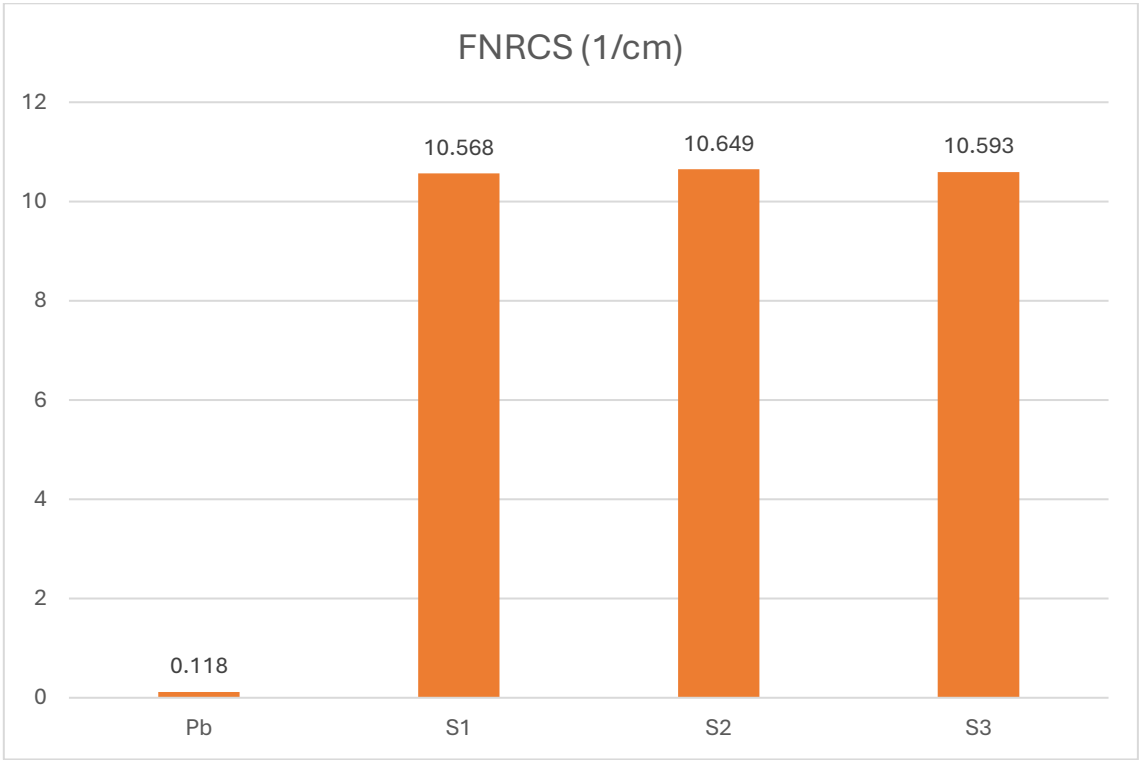


Figure 6. *FNRCS parameters for every samples*

Table 2. *G-P Fitting Parameters for EBF (S1)*

Energy	a	b	c	d	Xk
MeV					
1,50x10^{-2}	0,247	1,009	0,420	-0,152	8,674
2,00 x10^{-2}	0,472	1,013	0,235	-0,437	11,222
3,00 x10^{-2}	0,195	1,032	0,374	-0,289	26,857
4,00 x10^{-2}	0,248	1,059	0,336	-0,119	11,670
5,00 x10^{-2}	0,234	1,093	0,363	-0,137	13,771
6,00 x10^{-2}	0,219	1,133	0,389	-0,122	13,921
8,00 x10^{-2}	0,188	1,214	0,454	-0,106	14,135
1,00 x10^{-1}	0,512	1,291	0,164	-0,248	13,772
1,50 x10^{-1}	0,260	1,223	0,356	-0,143	14,036
2,00 x10^{-1}	0,171	1,269	0,501	-0,092	14,608
3,00 x10^{-1}	0,110	1,388	0,635	-0,052	14,161
4,00 x10^{-1}	0,072	1,495	0,765	-0,045	14,134
5,00 x10^{-1}	0,050	1,562	0,844	-0,037	14,076
6,00 x10^{-1}	0,032	1,595	0,904	-0,027	13,926
8,00 x10^{-1}	0,016	1,635	0,966	-0,021	13,871
1,00	0,008	1,641	1,000	-0,019	13,329
1,50	-0,020	1,566	1,116	-0,005	14,219
2,00	-0,021	1,601	1,127	-0,005	12,614
3,00	-0,004	1,614	1,059	-0,015	12,241
4,00	0,005	1,555	1,024	-0,019	12,836
5,00	0,013	1,493	0,999	-0,025	13,156
6,00	0,023	1,452	0,970	-0,032	13,266
8,00	0,031	1,371	0,950	-0,038	13,550
1,00 x10^{1}	0,038	1,311	0,936	-0,044	13,652
1,50 x10^{1}	0,050	1,218	0,919	-0,055	13,940

Table 3. *G-P Fitting Parameters for EBF (S2)*

Energy	a	b	c	d	Xk
MeV					
1,50 x10^{-2}	0,166	1,008	0,483	-0,052	8,087
2,00 x10^{-2}	0,363	1,014	0,312	-0,306	11,098
3,00 x10^{-2}	0,204	1,039	0,373	-0,239	22,306
4,00 x10^{-2}	0,244	1,077	0,344	-0,123	12,299
5,00 x10^{-2}	0,229	1,121	0,373	-0,132	14,033
6,00 x10^{-2}	0,206	1,167	0,410	-0,114	14,178
8,00 x10^{-2}	0,477	1,423	0,242	-0,182	14,183
1,00 x10^{-1}	0,379	1,211	0,246	-0,192	13,759
1,50 x10^{-1}	0,223	1,231	0,413	-0,121	14,201
2,00 x10^{-1}	0,172	1,345	0,506	-0,095	14,490
3,00 x10^{-1}	0,100	1,447	0,667	-0,048	14,290
4,00 x10^{-1}	0,061	1,556	0,802	-0,041	14,145
5,00 x10^{-1}	0,041	1,622	0,879	-0,035	14,081
6,00 x10^{-1}	0,023	1,651	0,938	-0,025	14,017
8,00 x10^{-1}	0,008	1,682	0,999	-0,018	14,087
1,00	0,001	1,683	1,027	-0,016	13,425
1,50	-0,024	1,588	1,135	-0,003	11,907
2,00	-0,021	1,627	1,125	-0,005	11,604
3,00	-0,005	1,625	1,059	-0,014	12,043
4,00	0,006	1,562	1,019	-0,018	12,542
5,00	0,014	1,501	0,991	-0,024	13,183
6,00	0,023	1,457	0,964	-0,031	13,215
8,00	0,032	1,377	0,941	-0,037	13,511
1,00 x10^{1}	0,038	1,315	0,930	-0,043	13,559
1,50 x10^{1}	0,047	1,218	0,920	-0,052	13,508

Table 4. *G-P Fitting Parameters for EBF (S3)*

Energy	a	b	c	d	Xk
MeV					
1,50 x10^{-2}	0,220	1,009	0,442	-0,118	8,475
2,00 x10^{-2}	0,438	1,014	0,259	-0,396	11,183
3,00 x10^{-2}	0,198	1,034	0,374	-0,273	25,435
4,00 x10^{-2}	0,247	1,064	0,338	-0,120	11,866
5,00 x10^{-2}	0,232	1,099	0,366	-0,135	13,992
6,00 x10^{-2}	0,214	1,140	0,397	-0,118	14,045
8,00 x10^{-2}	0,278	1,260	0,384	-0,131	14,035
1,00 x10^{-1}	0,470	1,265	0,190	-0,231	13,768
1,50 x10^{-1}	0,248	1,225	0,374	-0,136	14,088
2,00 x10^{-1}	0,171	1,293	0,502	-0,093	14,571
3,00 x10^{-1}	0,107	1,402	0,645	-0,050	14,220
4,00 x10^{-1}	0,068	1,513	0,776	-0,044	14,137
5,00 x10^{-1}	0,047	1,581	0,855	-0,037	14,070
6,00 x10^{-1}	0,029	1,612	0,914	-0,027	13,958
8,00 x10^{-1}	0,013	1,649	0,976	-0,020	13,938
1,00	0,006	1,654	1,008	-0,018	13,359
1,50	-0,021	1,572	1,124	-0,004	14,021
2,00	-0,021	1,609	1,126	-0,005	12,300
3,00	-0,004	1,618	1,059	-0,014	12,182
4,00	0,005	1,558	1,022	-0,019	12,740
5,00	0,013	1,495	0,996	-0,024	13,165
6,00	0,023	1,453	0,968	-0,032	13,249
8,00	0,031	1,373	0,948	-0,037	13,539
1,00 x10^{1}	0,037	1,312	0,935	-0,043	13,621
1,50 x10^{1}	0,050	1,219	0,916	-0,055	13,875

3. COST ASSESSMENT

In this study, theoretical lead panel for 1m^2 area and 0,5 cm thickness for comparison purposes and 2nd sample (70% epoxy + 15% Bi_2O_3 + 15% Ta_2O_5) is calculated.

The reason for choosing sample number 1 is that it shows good shielding around 70-90 keV thanks to the Ta_2O_5 contribution; Although it gives very close performance to the number 3 sample, it is thought to be more reasonable in terms of cost because the Ta_2O_5 rate is lower.

The reason for choosing the thickness of 0,5 cm was chosen according to the HVL and TVL graphics. This thickness provides a safer design, especially on the high energy side.

1m^2 for the panel calculation;

A= 1m^2, t= 0,5cm

V = 1000*0.5=5000cm^3

1. If we consider the density of the sample as 1.62g/cm^3, the total mass;

m = 1.62*5000=8100g

The mass and composition rates of the components are presented in Table 5.

Table 5. *Material Distribution*

Material	Rate	Mass
Epoxy	70%	5,67 kg
Bi_2O_3	15%	1,22 kg
Ta_2O_5	15%	1,22 kg
Total	100%	8,1 kg

Total Cost= $5.67*P_{epoxy}+1.22*P_{Bi2O3}+1.22*P_{Ta2O5}$

Here P values are explained as USD/kg. The unit and total costs of the components are presented in Table 6.

Table 6. *Cost calculation of Sample 2*

Material	Mass	Unit Price	Cost
Epoxy	5,67 kg	8,7 USD/kg	49,3 USD
Bi_2O_3	1,22 kg	128 USD/kg	156,16 USD
Ta_2O_5	1,22 kg	177 USD/kg	215,94 USD
Total	8,1 kg		421,4 USD

According to this cost calculation, the cost of the 2nd sample for 1m^2 area and 0,5 cm thickness is calculated as 421,4 USD. The cost calculation of the lead panel depending on the same conditions is made below.

1m^2, 0,5 cm for lead panel

$$\rho = 11.34\ g/cm^3$$

$$V = 10000 * 0{,}5 = 5000 cm^3$$

$$m = 5000 * 11{,}34 = 56.700 g$$

Judging by the current lead prices, it is used in the cost calculation as 1,98 USD/kg. The total cost of the lead panel is calculated as 112,3 USD. If labor, coating, supplier profit are added to these prices, the resulting price ranges are summarized in Table 7.

Table 7. *Cost comparison of lead and S2 sample*

Material	Thickness	Mass	Approximate Cost
Lead	0,5	56,7 kg/m^3	100-175 USD/m^3
2nd Sample	0,5	8,1 kg/m^3	400-450 USD/m^3

When we look at the cost table, the lead is about 7 times heavier and 3 times more than the 2nd sample. Is cheap. However, lead is toxic and harmful to the environment. It can also be said that lead can pose a danger to the environment not only during the use phase, but also during its production, processing, transportation and disposal. If this material is eroded over time or has a physical damage, it is possible for it to become a source of toxic particles and heavy metal ions by the environment. At the same time, it is seen that the use of portable systems is limited because the bullet-based shield systems are very heavy materials due to the density. As a result of this study, theoretically calculated 1 m area and 0,5 cm It is understood that 56,7 kg of toxic heavy metal is formed from a lead panel with a thickness. The epoxy/Bi_2O_3/Ta_2O_5 composite structure, which is recommended to be compared, has a mass of 8,1 kg and is an alternative to lead with its safer and more environmentally friendly structure.

4. CONCLUSION AND DISCUSSION

In this study, the radiation shielding performances of composite structures developed by adding Bi_2O_3 and Ta_2O_5additives in different proportions to the epoxy matrix were theoretically examined. The results obtained showed that tantalum oxide contribution provides significant advantages in the medium energy region. The increase observed in the energy range of 70-90 keV in MAC and LAC parameters was associated with the K-absorption edge of the tantalum at the level of approximately 67.4 keV. This reveals that composites with Ta_2O_5 doped improve the performance of radiation attenuation by increasing the possibility of photoelectric interaction.

In addition, Compton scattering becomes dominant at higher energy levels. It has been observed that all samples exhibit similar behaviors due to HVL, TVL and MFP. The G-P fitting parameters and buildup factor calculations employed in this study follow the methodology established by Singh and Badiger (2015). Harima (1983), ensuring consistency with the literature for evaluating multiple scattering effects. When the results are evaluated, it is understood that the attenuation capability weakens at higher energies (Kaçal et al., 2019). Especially S2 and S3 samples balanced shielding he drew attention thanks to his behavior. S3 sample is theoretically the highest shielding Although it is close to its performance, it has been evaluated that the S2 sample is more suitable in terms of optimal design due to its high tantalum cost. Therefore, 70% epoxy, 15% Bi_2O_3 S2 composite, which contains 15% Ta_2O_5, stood out as the most suitable structure in terms of performance and cost. Muthamma et al. (2020) previously reported that epoxy-Ta_2O_5-Bi_2O_3 composites exhibit enhanced attenuation properties at 59.54 and 662 keV, consistent with the present findings where the Ta_2O_5 contribution improves shielding performance in the medium energy range. FNRCS analyzes positively improve the neutron shielding performance of the tantalum contribution. It shows that it affects. As the tantalum ratio increases, the rapid neutron removal section is regularly Elevation, He confirms that he is. This result is that the developed composites are not only gamma rays, It also shows that there may be a potential alternative to neutron radiation.

Thus, the way is opened for new generation composite designs for multi-purpose radiation shielding applications. As emphasized in recent comprehensive reviews (More et al., 2021), the development of polymer-based composite materials for radiation shielding has gained significant momentum due to their lightweight nature, design flexibility, and environmental safety. Looking at the cost analyses, it is seen that the proposed composite structures are more expensive than lead. However, the disadvantages of lead-based shields such as high density, toxicity and environmental risks make it necessary to search for alternative materials. The S2 composite has a mass of approximately 8,1 kg/m3, while the lead panel of the same size is approximately 56,7 kg. This shows that the developed structure offers an important advantage of lightness. This can provide a significant engineering advantage, especially in terms of portable radiation protection systems, medical equipment, mobile imaging devices and aviation applications. In addition, the fact that epoxy/ Bi_2O_3/Ta_2O_5 composites does not contain toxic heavy metals constitutes an important advantage in terms of environmental sustainability and human health.

As a result, it has been seen that epoxy composites with Bi_2O_3 and Ta_2O_5 doped offer a powerful alternative to lead-free radiation armouring materials. It has been determined that hybrid composites exhibit more controlled and broad-spectrum armouring behavior, especially thanks to the contribution of tantalum contribution in the medium energy region. However, since this study is based on theoretical analysis, experimental verification studies should be carried out in the future. Experimental examination of parameters such as mechanical strength, thermal stability, long-term radiation resistance and optimization of production processes is critical for the transfer of these composites to real applications. Erdogan et al. (2025) similarly emphasized that

radiation interaction characterization should extend beyond photon parameters to include electron and ion interactions, supporting the multidimensional approach adopted in the present study. Furthermore, recent advances in additive manufacturing techniques, such as the DLP 3D printing of bio-based photopolymer–colemanite composites (Eken et al., 2026), suggest that the production of complex-shaped, lightweight shielding components with customized properties is increasingly feasible, offering a pathway for the practical implementation of the composites developed in this study. Thus, this work can contribute to the development of environmentally friendly, lightweight and high-performance new generation radiation shielding systems (More et al., 2021).

AUTHOR CONTRIBUTIONS

S.S.K.: Investigation, Formal Analysis, Manuscript – Original Draft, Resources. E.C.H.: Software, Visualization, Analysis and Interpretation, Editing. S.B.O.: Conceptualization, Supervision, Methodology, Formal Analysis, Review, Validation.

AI Exclusion: AI tools are strictly prohibited from being listed as authors.

Legal Consent: All human authors confirm they have reviewed and legally accepted the final version under the **CC BY-SA 4.0** framework.

CONFLICT OF INTEREST

The authors declare no conflict of interest.

REFERENCES

Eken, S., Kavun, Y., Çelikçi, N., & Kerli, S. (2026). Production of bio-based Photopolymer–Colemanite resin composites using 3D DLP printing for advanced radiation protection. *Applied Radiation and Isotopes*, *229*, 112380. https://doi.org/10.1016/j.apradiso.2025.112380

Erdogan, T., Eken, S., & Sahin, M. C. (2025). Theoretical investigation of radiation absorption properties of electrons, photons, and heavy ions in Fe-based shape memory biomedical alloys. *Radiation Effects and Defects in Solids*, 1-16. https://doi.org/10.1080/10420150.2025.2562527

Harima, Y. (1983). An approximation of gamma-ray buildup factors by modified geometrical progression. *Nuclear Science and Engineering, 83*(2), 299-309. https://doi.org/10.13182/NSE83-A18222

Kaçal, M. R., Akman, F., Sayyed, M. I., & Akman, F. (2019). Evaluation of gamma-ray and neutron attenuation properties of some polymers. *Nuclear Engineering and Technology, 51*(3), 818-824. https://doi.org/10.1016/j.net.2018.11.011

Khasanov, S., Temirov, J., & Tashmetov, M. (2026). Bismuth oxide-based lead-free radiation shielding materials: A cross-matrix review. *Radiation Physics and Chemistry, 248*, 114122. https://doi.org/10.1016/j.radphyschem.2026.114122

Kim, J., Bar-Ness, D., Si-Mohamed, S., Coulon, P., Blevis, I., Douek, P., & Cormode, D. P. (2018). Assessment of candidate elements for development of spectral photon-counting CT specific contrast agents. *Scientific Reports*, *8,* 12119. https://doi.org/10.1038/s41598-018-30570-y

Knoll, G. F. (2010). *Radiation Detection and Measurement*.

Landsberger, S., Hashem, J., Phathanapirom, B., Williams, J., & Cournoyer, M. (2011). Photon attenuation in non-leaded gloves. *Transactions of the American Nuclear Society*, *104*, 625-627.

Lin, H.-N., Lin, C.-K., Chang, P.-j., Chang, W.-M., Fang, A., Chen, C.-Y., Yu, C.-C., & Lee, P.-Y. (2021). Effect of tantalum pentoxide addition on the radiopacity performance of Bi_2O_3/Ta_2O_5 composite powders prepared by mechanical milling. *Materials*, *14*(23), 7447. https://doi.org/10.3390/ma14237447

More, C. V., Alsayed, Z., Badawi, Mohamed. S., Thabet, Abouzeid. A., & Pawar, P. P. (2021). Polymeric composite materials for radiation shielding: A review. *Environmental Chemistry Letters, 19*(3), 2057-2090. https://doi.org/10.1007/s10311-021-01189-9

Muthamma, M. V., Bubbly, S. G., & Gudennavar, S. B. (2020). Attenuation properties of epoxy-Ta_2O_5 and epoxy-Ta_2O_5-Bi_2O_3 composites at γ-ray energies 59.54 and 662 keV. *Journal of Applied Polymer Science, 137*(44), 49366. https://doi.org/10.1002/app.49366

Nuñez-Briones, A. G., Benavides, R., Bolaina-Lorenzo, E. D., Martínez-Pardo, M. E., Kotzian-Pereira-Benavides, C., Mendoza-Mendoza, E., Betancourt-Galindo, R., & Garcia-Cerda, L. A. (2023). Nontoxic flexible PVC nanocomposites with Ta_2O_5 and Bi_2O_3 nanoparticles for shielding diagnostic X-rays. *Radiation Physics and Chemistry, 202*, 110512. https://doi.org/10.1016/j.radphyschem.2022.110512

Singh, V. P., & Badiger, N. M. (2015). Gamma Photon Exposure Buildup Factors for Some Spin Ice Compounds Using G-P Fitting Method. *Journal of Nuclear Physics, Material Sciences, Radiation and Applications, 2*(2), 169-179. https://doi.org/10.15415/jnp.2015.22013

Şakar, E., Özpolat, Ö. F., Alım, B., Sayyed, M. I., & Kurudirek, M. (2020). Phy-X / PSD: Development of a user friendly online software for calculation of parameters relevant to radiation shielding and dosimetry. *Radiation Physics and Chemistry*, *166*, 108496. https://doi.org/10.1016/j.radphyschem.2019.108496

Zhang, X., Chen, Q., & Zhang, S. (2021). Ta_2O_5 Nanocrystals Strengthened Mechanical, Magnetic, and Radiation Shielding Properties of Heavy Metal Oxide Glass. *Molecules*, *26*(15), 4494. https://doi.org/10.3390/molecules26154494